International Journal of Hydrogen Energy 128 (2025) 306–318

Contents lists available at ScienceDirect

International Journal of Hydrogen Energy

journal homepage: www.elsevier.com/locate/he

Experimental analysis on a Power-to-Hydrogen system based on PEM electrolysis and metal hydrides: Empirical correlations for optimal system design and performance improvement

Riccardo Alleori [a], Maria Alessandra Ancona [b], Michele Bianchi [b], Francesco Falcetelli [b], Federico Ferrari [b,*], Francesco Melino [b], Paolo Pilati [c], Mattia Ricco [c]

[a] Alma Mater Studiorum Università di Bologna, Inter-Departmental Center for Industrial Research on Renewable Sources, Environment, Sea and Energy (CIRI-FRAME), Via Zamboni 33, 40131, Bologna, Italy
[b] Alma Mater Studiorum Università di Bologna, Department of Industrial Engineering (DIN), Viale del Risorgimento 2, 40136, Bologna, Italy
[c] Alma Mater Studiorum Università di Bologna, Department of Electrical, Electronic and Information Engineering (DEI), Viale del Risorgimento 2, 40136, Bologna, Italy

ARTICLE INFO

Keywords:
Metal hydrides
Hydrogen storage
PEM electrolyzer
Power-to-Gas

ABSTRACT

Metal Hydrides (MH) represent a promising technology for hydrogen storage, traditionally characterized using Pressure-Composition-Temperature (PCT) diagrams. However, real-world applications introduce additional complexities, such as non-equilibrium conditions driven by fluctuating hydrogen production rates and the chemical kinetics of MH materials. These factors necessitate dynamic response studies to optimize storage strategies, particularly in the context of renewable energy integration. This study investigates a Power-to-Hydrogen (P2H) system coupling a 2.5 kW Proton Exchange Membrane (PEM) electrolyzer with AB2-type MH canisters (190 NL or 800 NL), a configuration that remains underexplored in current literature but aligns with practical application scenarios. The experimental campaign focuses on key aspects: the influence of MH storage size, the impact of thermal conditioning on storage performance, and the operational dynamics of the hydrogen generator, with particular attention to hydrogen venting and current ripple phenomena. Results show that the 800 NL canister allows a better coupling with the considered electrolyzer (119 g of stored hydrogen corresponding to 6.35 kWh of stack consumption in the best case) and a mean stack efficiency of 61.4 % can be achieved with thermal conditioning (water cooling to maintain 20 °C during the adsorption phase). Overall, the findings provide critical insights into optimizing the PEM electrolyzer-MH tank interaction under real-world conditions, offering guidance for improving hydrogen storage system efficiency. This work contributes to advancing hydrogen-based energy storage systems, enhancing their role in supporting renewable power integration and promoting energy sustainability.

1. Introduction

Nowadays, hydrogen is mainly produced using fossil fuel technologies without emissions controls. In the Net Zero Emissions by 2050 Scenario, hydrogen becomes crucial for decarbonizing difficult sectors like heavy industry and long-distance transport, with renewable electricity-powered electrolysis being the primary method of production [1]. Hydrogen can act as an energy buffer and improve the long-term stability of the power grid by balancing demand and availability of electric power according to the principles behind systems called Power to Hydrogen to Power (P2H2P). Such systems belong to the broader set of Power to Gas to Power (P2G2P) and involve the transfer of a form of energy to hydrogen, which stores it in the form of bonding energy, followed by storage of the H_2 molecule, its transport, and finally reconversion to useful energy [2]. Water electrolysis for hydrogen production is not a new technology, with industrial-scale units exceeding 100 MWe installed as early as the first half of the 20th century. According to the International Energy Agency (IEA), global installed capacity reached about 5.2 GWe by 2024 [3]. IEA data shows that approximately 71 % of global operational capacity uses alkaline electrolysis, while 20 % uses proton exchange membrane (PEM) electrolysis. In Europe, the distribution is more balanced, with alkaline systems accounting for 44 % and

* Corresponding author.
E-mail address: federico.ferrari28@unibo.it (F. Ferrari).

https://doi.org/10.1016/j.ijhydene.2025.04.201
Received 20 January 2025; Received in revised form 2 April 2025; Accepted 10 April 2025
Available online 16 April 2025

PEM for 53 %, thanks to several recently commissioned large PEM projects. Both technologies are considered mature, rated at technology readiness level (TRL) 9, and have achieved commercial operation in relevant environments, as per IEA standards [4]. These two low temperature-based technologies are opposed by high-temperature electrolysis based on solid oxide cells, where a ceramic electrolyte enables the transport of oxide ions (O_2^-). Solid oxide electrolyzer cells (SOEC) are at an advanced stage of research and development and show great potential for promising high levels of efficiency [5]. In addition to low-temperature-based technology, another type of electrolyzer is anion exchange membrane which can be regarded as compromise between PEM and alkaline hydrogen generators. This technology enables operation at higher current densities, thereby increasing hydrogen production, making it more comparable to PEM electrolyzers. However, it offers a cost advantage by eliminating the need for expensive membranes, catalysts and plates because it does not work in acidic conditions like PEM [6].

However, regardless of the technology employed, one of the main challenges to the deployment of hydrogen as an alternative fuel is storage [7]. Indeed, this is still an open technological challenge more than ever nowadays, as the main systems currently deployed at the industrial level have several critical issues.

With regard to compressed hydrogen, the best technology on the market utilizes cylinders made from materials with exceptionally high mechanical properties, enabling pressures of up to 800 bar and ensuring storage capacities of 43.39 kg_{H2}/m^3 [8]. It is also possible to store hydrogen in a liquid state using cryogenic systems operating at temperatures below −253 °C, obtaining storage capacities of about 71.0 kg_{H2}/m^3. However, boil-off phenomena associated with the evaporation of hydrogen from tanks must be carefully managed to prevent excessive pressure buildup, which could lead to hydrogen venting once the maximum tank pressure is reached [9,10].

Recently, hydrogen storage systems using metal hydrides are being investigated, since they can offer numerous advantages compared to gas compression or liquefaction in terms of safety and performance [2]. Although the discovery of these compounds dates back to as far as 1869, the first applications in the energy field did not occur until the 1960s and 1970s. This promising form of storage allows for high volume energy density (up to 4 kWh/dm^3 corresponding to approximately 120 kg_{H2}/m^3 of hydrogen) [11], operating at relatively low pressures. The adsorption phase requires proper thermal management to maintain temperature low due to the exothermal nature of chemical reaction [12]. On the other hand, high operating temperatures are often required to achieve high energy release efficiency, a condition that can prove particularly energy-intensive [13,14]. There are three categories of metal hydrides: elemental, complex and interstitial, depending on the type of chemical compound formed [11].

Specifically, this study focuses on interstitial metal hydrides, which are generally non-stoichiometric compounds in which hydrogen becomes part of the crystal lattice of a metal or metal alloy. The acronyms AB, AB2 and AB5 are used to denote the elements present in greater quantities in the starting alloy and an approximation of their proportions within it. They generally have lower operating temperatures than elemental hydrides, ranging from −50 to 200 °C, and storage capacities for different alloys in the range of 2 % by weight [15]. More in detail, the efficiency of hydrogen storage in MH is traditionally evaluated through Pressure-Composition-Temperature (PCT) diagrams [16].

However, in practical scenarios, the performance evaluation of storage cannot be separated from the associated production technology. In the perspective of implementing a MH-based storage system in a real application, for example coupled with a PEM-E, there are additional factors that must be considered.

Even though storage is achieved at constant temperatures, for instance by employing a properly designed thermal conditioning system, it does not follow the corresponding PCT curve. Indeed, a PCT curve can be thought of as a series of points representing subsequent equilibrium conditions at different levels of hydrogen concentration. The equilibrium condition requires a certain amount of time which depends on the MH chemical kinetics. On the other hand, in real operational conditions, hydrogen is produced and sent to the storage system with flow rates that depend on available power and the control logic of the electrolyzer. In such conditions it becomes crucial to study the dynamic response of the system to develop an effective optimization strategy.

Concerning PEM-type electrolyzer, many studies are being conducted involving several fundamental aspects of this system. Among the most widely approached topics is certainly the numerical modeling of the stack [17], namely the component in which the electrolysis of water takes place. In particular, since these devices are designed to be coupled to renewable energy sources (RES), some models have focused on reproducing the dynamic behavior of the stack as the input current made available from the grid varies [18].

Since the electrolyzer is intended to be coupled to RESs, the presence of a power electronic converter is inevitable. Therefore, an additional aspect to which attention is to be brought in this paper concerns a particular phenomenon caused by the power electronics powering the stack: the current ripple. The ripple is a phenomenon caused by power electronic converters and consists of a voltage or current oscillation around their desired mean value. This oscillation can vary in amplitude and frequency, depending on the design parameters of the converter and the control techniques used. Generally, it is desired to contain the ripple within a certain threshold. The current ripple appears to have a degrading effect on the polymer membrane of PEM electrolyzers, and more in general of PEM cells. This is because fluctuations in the current cause fluctuations in the flow rates of the reagents, which can lead to mechanical stress on the membrane. Several studies have shown that ripple at low frequencies, in the order of hundreds of Hz, has a greater impact on the life of a cell than ripple at higher frequencies (thousands of Hz) [19–21]. Whereas, at the same frequency, the amplitude of the ripple is always directly proportional to the reduction in cell life. Furthermore, ripple appears to cause a decrease in conversion efficiency, even for high frequencies [22,23].

In light of the aforementioned discussion, the aim of the present work is to focus on the direct coupling between PEM electrolyzer and MH tanks to analyze the behavior of a commercial hydrogen generator and its balance of plant (BoP), varying the operating conditions.

The experimental campaign conducted in this work aims to.

i. Study the influence of storage size (MH) in coupling with a 2.5 kWe nominal power PEM electrolyzer (PEM-E);
ii. Analyze the behavior of the hydrogen generator as the thermal conditioning of hydride canisters changes;
iii. Deepen the study of the electrolyzer with particular interest in the dynamics of the H2 vent and the phenomenon of current ripple.

In detail, the tests investigated the production of hydrogen by means of an electrolyzer of medium-sized PEM technology, powered directly from the electricity grid, which conveys the flow of hydrogen in a storage system consisting of metal hydride cylinders of type AB2 (based on TiMg alloy) [24].

2. Methods

2.1. Test bench description

The layout of the test bench is represented in Fig. 1: it consists of a Power-to-Gas (P2G) system based on a PEM-E which produces and sends hydrogen to two MH canisters. Since the adsorption phase is an exothermic reaction, the test bench is integrated with a thermal conditioning system used to cool down the MH canisters during the charging phase.

In more detail, the current experimental set-up is composed of.

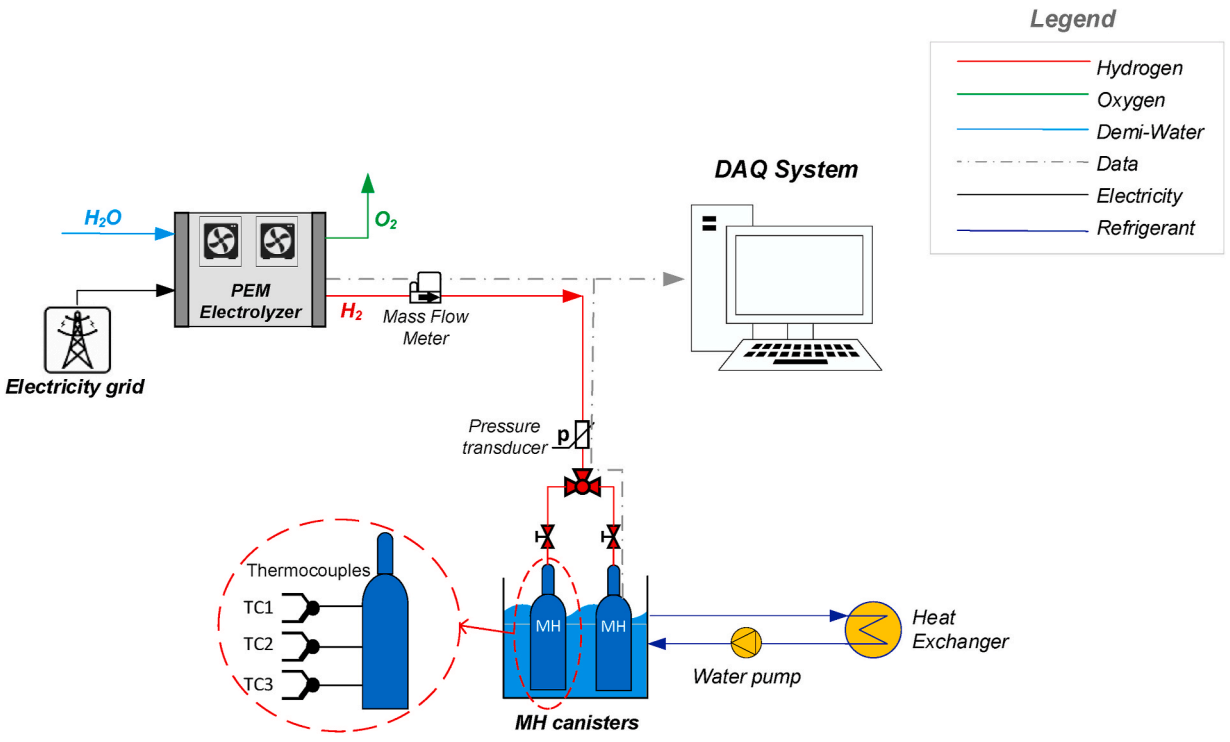

Fig. 1. Test bench layout.

i. A PEM electrolyzer, able to produce about 44.5 g/h (500 NL/h) of hydrogen at 15 bar, with a rated power consumption of 2.5 kW (AC), which corresponds to an efficiency of approximately 60 % taking as reference the hydrogen LHV;
ii. A hydrogen storage system, namely MH canisters in two different sizes: the first one is able to store 71.2 g (800 NL) of hydrogen at a maximum pressure of 25 bar in a physical volume of 2 L (corresponding to approximately 1.2 kWh/L taking as reference the hydrogen LHV), while the second one can store at most 16.9 g (about 190 NL) of hydrogen at a maximum pressure of 10 bar in a physical volume of 0.5 L (corresponding to approximately 1.1 kWh/L taking as reference the hydrogen LHV);
iii. A water-cooling circuit as thermal conditioning system for the MH canisters consisting of a centrifugal water pump, a thermal buffer tank and a self-built water-bath heat-exchanger;
iv. A Data Acquisition and Control (DAQ) system developed in Matlab™ environment and based on Arduino™ hardware, able to communicate with the electrolyzer's PLC (Programmable Logic Controller);
v. The system has been equipped with transducers and sensors to monitor the main thermodynamic quantities (such as pressures, flow rates and temperatures). A summary table of the measurement points on the plant is given in Table 1.

2.2. Design of experiment

This study considers a total of three experiments carried out under the conditions shown in Table 2.

The first part of this study is focused on two analyses based on experimental data, both aimed at examining the behavior of the PEM-E under several operating conditions.

The target of the first analysis was to investigate the effect of storage size on hydrogen production by the electrolyzer. In this regard, the

Table 2
Design of experiment.

	Test	Canister size	Cooling Fluid	Ambient Temperature (max. Variation ±2 °C)	Set point Pressure
MH tanks size effect	#1	2 × 190 NL	Air	21 °C	10 bar
	#2	2 × 800 NL	Air	23 °C	15 bar
MH tanks cooling effect	#2	2 × 800 NL	Air	23 °C	15 bar
	#3	2 × 800 NL	Water	21 °C	15 bar

Table 1
Investigated physical quantities and corresponding sensors installed in the test bench.

Physical quantity	Symbol	Unit	Sensor	Accuracy	Measuring range	Output signal
H_2 delivery pressure (to canisters)	p_{H2}	bar	Pressure transducer	±0.25 FS	0 ÷ 15 bar	0 ÷ 10 V
H_2 delivery mass flow	$\dot{m}_{H2}$	NL/min	Thermal mass flow meter	±0.5 % FS	0.1 ÷ 85 NL/min	4 ÷ 20 mA
Ambient temperature	T_{amb}	°C	T-type thermocouple	±0.5 °C	−20 ÷ 350 °C	TC
Heat-exchanger chamber water temperature	$T_{water\text{-}HX}$	°C	T-type thermocouple	±0.5 °C	−20 ÷ 350 °C	TC
Surface canister temperature (top)	T_{top}	°C	K-type thermocouple	±0.5 °C	−75 ÷ 250 °C	TC
Surface canister temperature (middle)	T_{middle}	°C	K-type thermocouple	±0.5 °C	−75 ÷ 250 °C	TC
Surface canister temperature (bottom)	T_{bottom}	°C	K-type thermocouple	±0.5 °C	−75 ÷ 250 °C	TC
Stack voltage	V_{stack}	V	Differential voltage probe	±2 % measure	−70 ÷ 70 V peak	−7 ÷ 7 V
Stack current	I_{stack}	A	DC/AC current probe	±4 % measure + 50 mA	0 ÷ 100 A peak	100 mV/A

adsorption test has been carried out with tanks in air at a temperature in the range of 21 °C and 23 °C, by varying the size of the storage: in test #1 two canisters with a maximum capacity of 190 NL at 10 bar were used, instead in test #2, two canisters with a maximum capacity of 800 NL each were used at a maximum pressure of 15 bar. In test #1 the maximum pressure at which the test was conducted is driven by the maximum pressure at which the hydride canister can operate. In contrast, the canisters in test #2 and test #3 can operates up to 25 bar, therefore the maximum filling pressure was chosen considering the production capacity of the PEM-E, which can produce hydrogen at a maximum of 15 bar.

The second analysis focuses on the cooling effect of MH-tanks. In fact, the adsorption process of MH is an exothermic reaction which involves the raising of the temperature of the metallic powder and the consequent loss of efficiency of the process [16]. In this context, a comparison between test #2 and test #3 has been introduced: indeed, the latter was carried out by using the same size of MH canisters but utilizing water within a cooling circuit to keep the temperature of the canisters as constant as possible.

For each test, the approach adopted consisted of a control strategy for the electrolyzer operating under a floating load and pressure-based system. This strategy is based on the capability of the generator to operate at partial loads in response to the thermodynamics dictated by the hydrogen adsorption process, halting production once the maximum allowable pressure of the MH tanks (as specified in the technical data sheet) is reached. Additionally, there were no constraints on the available electrical power from the grid, letting the electrolyzer free to vary the flow rate of hydrogen to be sent to the canisters.

In both analyses several parameters are investigated: the stack power and some thermodynamics parameters such as pressure and the hydrogen mass flow. Finally, there are also some energy considerations as a result of the stack efficiency calculation, which is LHV based as is shown in the following equation:

$$\eta = \frac{m_{H2} \cdot LHV}{E_{stack}} \tag{1}$$

Where m_{H2} is the mass of hydrogen produced and E_{stack} is the electric energy consumption of the stack, namely excluding auxiliaries.

The second part of the work focuses on a deeper characterization of the electrolyzer BoP, schematized in Fig. 2(a and b). The BoP can be thought as an assembly of three main subsystems, namely: the water management section (blue line), the oxygen (green line) and the hydrogen (red line) after-treatment sections. More in detail, the study focuses on dehumidification and purification processes of the hydrogen produced at the cathode side, analyzing the fluid path and the main control logic of the process to ensure a level of purity above 99.999 %. To this purpose, it is necessary to vent a small part of the hydrogen produced regularly. Specifically, leaving the cathode, wet hydrogen meets a splitter that operates also as buffer to stabilize the stack operation, and then is divided into two different flows: the first one, is sent to a filter cartridge and then to a gravimetric separation stage in which water is recovered from the bottom to be then recirculated at the anode by the water management subsystem; the second flow, characterized by a lower water content, is sent to a heat exchanger to allow further humidity condensation, removed by means of an additional gravimetric separator. Pure and dry hydrogen is finally spilled on the top of the same separator and supplied to the user.

Both the separation stages are responsible for the hydrogen vent since hydrogen and all the impurities are retained in the filters, while the water returns to the tank. However, the filters must be cleaned and reactivated constantly, which is why the hydrogen generator needs a control logic that allows it to open the purge valve. Moreover, hydrogen venting decreases the system efficiency because part of the hydrogen produced is lost. This problem is enhanced when the electrolyzer works at low loads, since the ratio between the hydrogen loss and the hydrogen sent to MH tanks is higher than the same quantity evaluated at high loads.

The last analysis presented in this work regards the current ripple to assess the phenomenon intensity caused by a real power electronic converter designed for this type of application.

A method, also proposed in other works, for quantifying the intensity of this phenomenon in a simple way can be by considering the ripple factor γ, i.e. the ratio between the rms value X_{rms} and the desired mean value X_m of the magnitude, as follows [25,26]:

$$\gamma = \frac{X_{rms}}{X_m} \tag{2}$$

If the ripple factor is bigger than 1, it means that ripple is present.

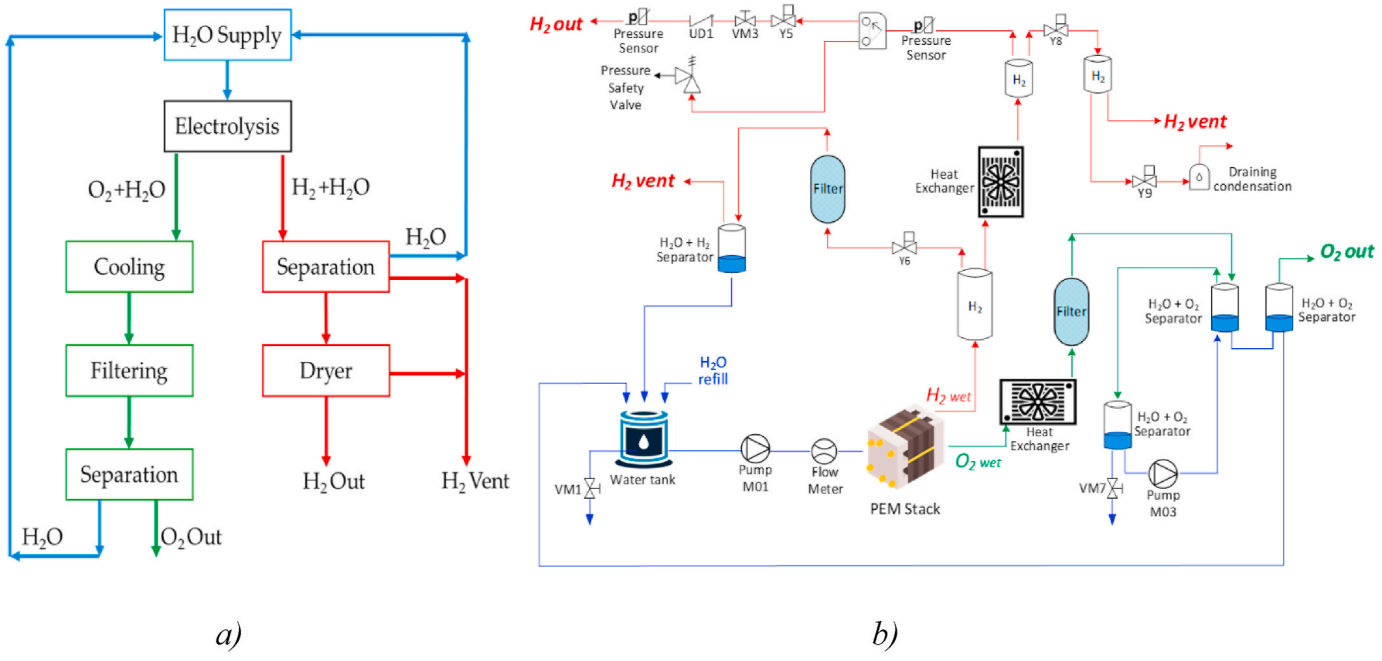

Fig. 2. Balance of Plant of the electrolyzer under investigation: conceptual workflow (a) and detailed scheme (b).

The greater the deviation from 1, the more severe the phenomenon is in amplitude.

3. Results

3.1. Investigation on effect of MH tanks size

3.1.1. Electrical parameters

Fig. 3(a and b) shows the electrical parameters of the stack electrolyzer monitored during test #1 carried out with the smaller canisters (190 NL). As can be seen from Fig. 3a, the load control is achieved by keeping the voltage unchanged and acting on the current sent to the stack. After an initial brief activation phase in which the maximum value of the power at which the stack can operates is reached (Fig. 3b), the rest of the test proceeds with minimal power absorption from the grid that remains almost constant until the end, where there is a slight improvement of the current in the last 30 min of the test. On the contrary, Fig. 3(c and d) shows the electrical parameters of the stack electrolyzer monitored during test #2 carried out with the larger canisters (800 NL). In comparison to test #1, after the activation phase the PEM-E operates at maximum load for approximately 25 min. Then, the current sent to the stack drops to 10 A after approximately 1 h of operation. After this phase, the current, and consequently the power adsorbed, decreased with a much lower rate compared to the previous phase, reaching a minimum value of around 5 A.

Hence, the MH size affect significantly the electrical parameters of the electrolyzer, considering that the boundary conditions were similar. In fact, the power adsorbed from the stack appears different from test #1 to test #2. Moreover, the duration of the tests is significantly different: test #1 lasted less than 2 h while test #2 ended after 6.5 h.

As can be seen from Fig. 3, in both system couplings, electric current peaks are evident due to the purge control logic of the electrolyzer, better assessed in the following section.

3.1.2. Thermodynamic parameters

This section focuses on two other physical quantities which are the fundamental object of study within this project: the pressure and flow rate of hydrogen sent to the storage vessels.

In Fig. 4a is shown the pressure trend detected during the test carried out by filling the 190 NL canisters (test #1). The pressure value has an exponential trend which stops when the set-point pressure (10 bar) is reached. On the other hand, the trend of the hydrogen flow is represented in Fig. 4b. Specifically, the hydrogen flow calculated by the PLC electrolyzer is represented by the pink line, whereas the one measured by the flow meter installed downstream of the generator is illustrated with the blue line. As it is possible to observe, the electrolyzer keeps the

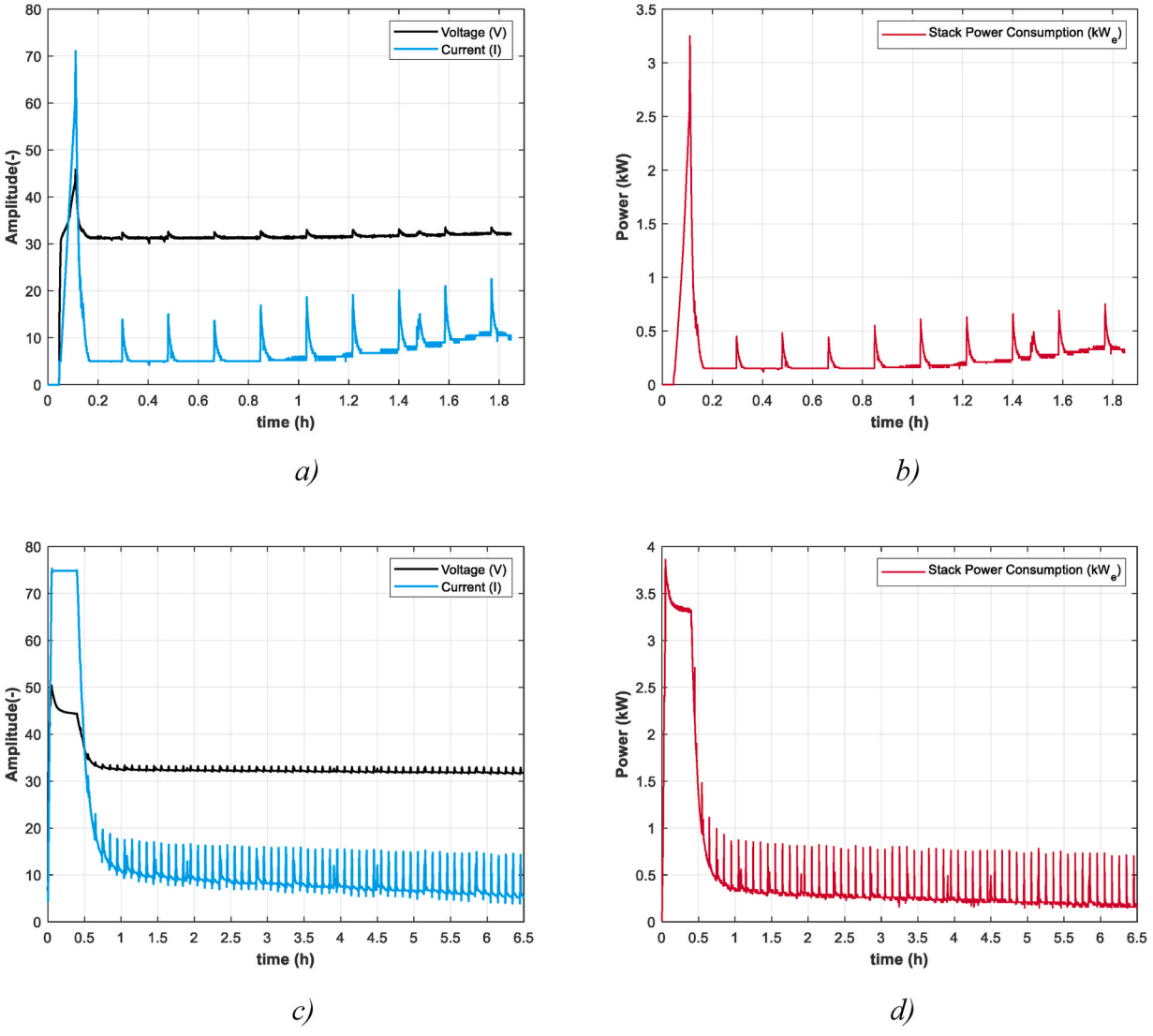

Fig. 3. Electrical parameters of the hydrogen generator monitored during test #1 and test #2.

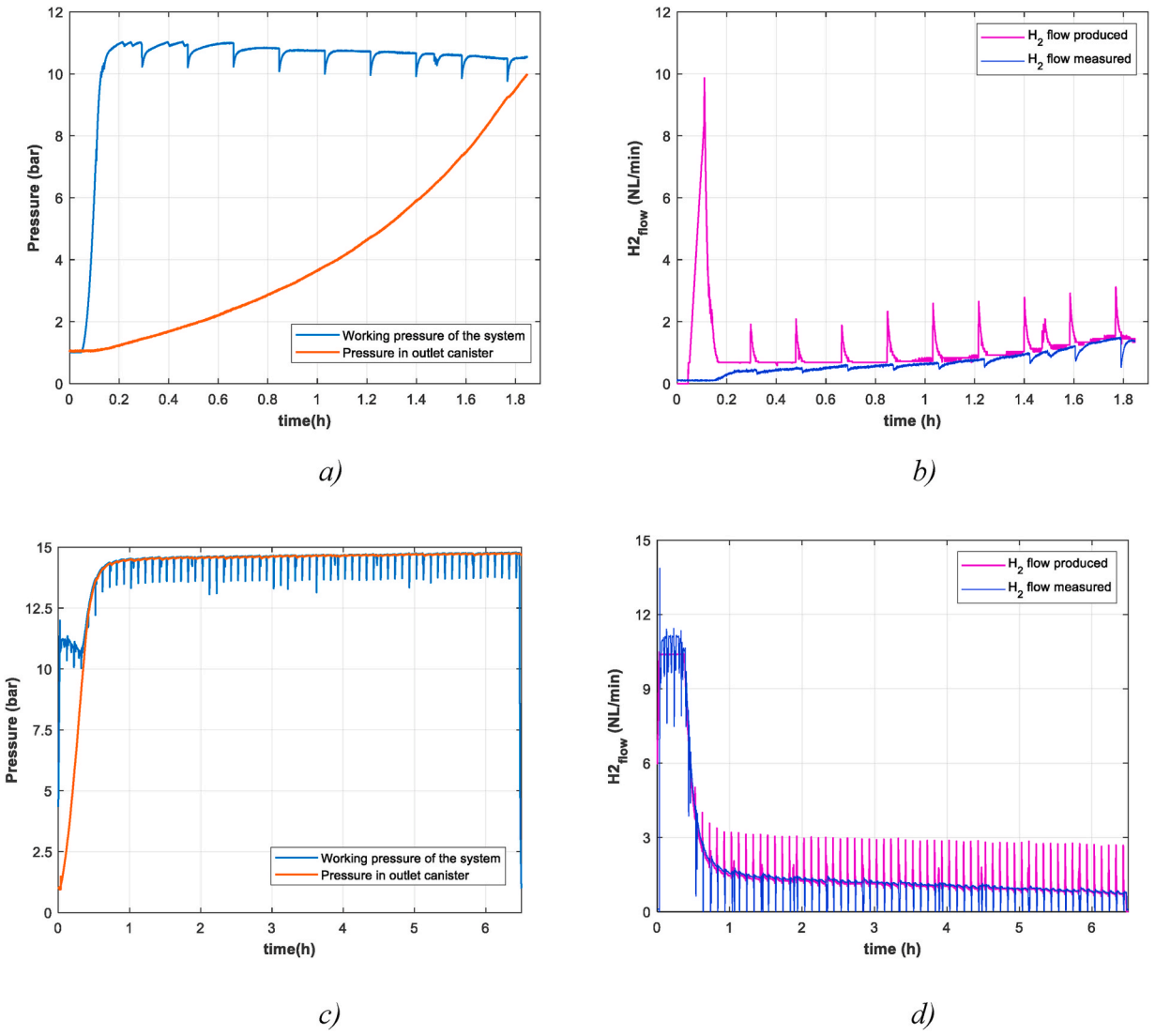

Fig. 4. Pressure and flow rate of the hydrogen produced by the generator during test #1 and test #2.

hydrogen flow at very low values (smaller than 1 NL/min) with a very slightly increasing trend. Although the flow is relatively low, not all the hydrogen sent to the canisters chemically binds; therefore, some of it is stored by compression, contributing to a rapid increase in pressure. Similarly, Fig. 4 (c, d) presents the same analysis related to the test carried out with the 800 NL canisters (test #2). The pressure and flow trends are completely different compared to the previous case, proving that the PEM-E is sensitive to the different sizes of MH tanks. The pressure increases rapidly in the first phase of the test, when the electrolyzer is operating at maximum load and delivering hydrogen with the highest flow value. Then, when the working pressure of the system and the pressure in the outlet canister become similar, the PEM-E drastically reduces the flow rate sent to the canisters. Therefore, as a direct consequence, the pressure growth slows down since in this case the MH alloy is capable of chemically adsorbing almost all the hydrogen entering the storage system, thus storing by compression only a small percentage of it. It results that the pressure slope (Fig. 4c) in the outlet canisters begin to flatten when there is about 1.5 bar of difference from the pressure set point, and, consequently, the hydrogen flow (Fig. 4d) begins to decrease very slowly after 1 h from the start until the end of the test.

3.1.3. *Stack efficiency*

The study of MH tanks size effect on the electrolyzer behavior ends with the comparison of stack efficiency during the tests, calculated by Eq. (1). In Fig. 5a is shown the efficiency curve of the stack for the test #1, while in Fig. 5b is shown the one related to the test #2. Both the figures have the same trend, which is coherent with other curves already present in the literature [26]. As was discussed earlier, during test #1 the stack operated exclusively by adsorbing minimum values of electrical power from the grid, therefore in those points where the efficiency is highest. In contrast, during test #2 the stack works at many more operating points, including those at 100 % load where the efficiency reaches values even below 60 %.

3.2. *Investigation on the effect of MH canister cooling*

The cooling of metal hydrides is a key aspect to counterbalance the exothermic nature of the adsorption reaction and allow the effective storage capacities of the canisters to be increased. In this comparison, test #2 and test #3 are analyzed; both tests utilize canisters of the same size (800 NL) and start from the same ambient temperature. However, in test #3, a thermal conditioning circuit is employed to maintain a constant surface temperature of the canisters.

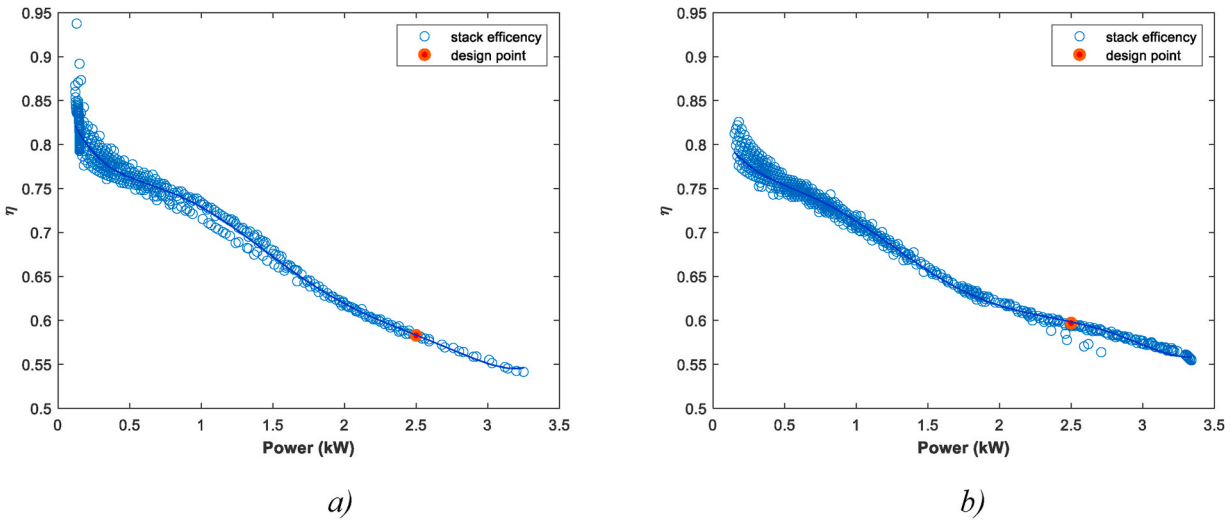

Fig. 5. Efficiency curve obtained from experimental data for test #1 (a) and test #2 (b).

3.2.1. Electrical parameters

Data regarding all the electrical parameters of interest measured in the test in circulating water (test #3) are shown in Fig. 6(a and b). The electrical behavior of the PEM-E is very similar to what was found in the test carried out in test #2 (Fig. 3c,d): in the first part of the test the stack operates at 100 % load, while for the remaining part this gradually decreases. However, two important differences can be noted. First, the time in which the electrolyzer adsorbs the maximum power from the grid extends for about 12 min longer than in the case in air. Second, in contrast to what was observed previously, the rate at which the load decreases is significantly less abrupt. This behavior can be attributed to the beneficial effect that thermal conditioning has on the canisters. In fact, by being able to cool the MH cylinders, it is possible to have greater control over the adsorption reaction, ensuring its higher efficiency. As a result, the resistance that the electrolyzer feels at discharge decreases, allowing it to work at higher loads. Finally, the test duration is also longer for test #3 than for test #2 differing by about 30 min.

3.2.2. Thermodynamic parameters

Observations from test #2, as shown in Fig. 4(c and d), reveal trends that, when compared to the pressure and flow patterns of hydrogen in test #3 depicted in Fig. 7(a and b), exhibit notable similarities. However, a deeper analysis shows that during test #3 the cooling of MH tanks has a consequence on the pressure trend. Indeed, compared to test #2, the curve begins to reduce its slope already at a Δp of about 3 bar from the set-point pressure, instead of 1.5 bar. Obviously, this difference is reflected also in the hydrogen flow, which decreases much more slowly than in test #2. This can be attributed to the fact that, at a controlled temperature of approximately 20 °C, the amount of hydrogen delivered to the metal hydride (MH) tanks is effectively adsorbed by the metal powder. This absorption facilitates a balance that results in only slight variations in the internal pressure of the canister, despite the relatively high flow rate, likely because the equilibrium pressure of the MH has been reached.

3.2.3. Energy assessment

As discussed previously, during test #3 the electrolyzer, due to the positive effect of cooling the MH canisters, was able to work for a longer period at a higher load than in test #2. Clearly, some important energy considerations about the studied system can be deduced from this condition. Voltage and current values at the stack have been measured during the tests to reproduce the polarization curve of the electrolyzer stack (Fig. 8a). The polarization curve of the stack is independent of the PEM-MH coupling, thus it is consistent across all three tests conducted.

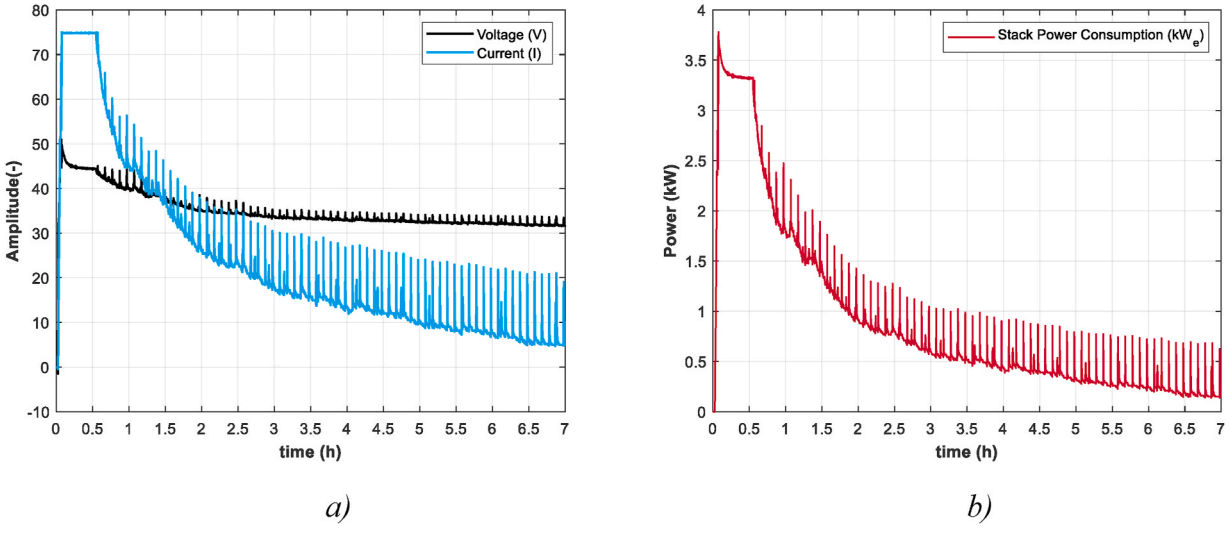

Fig. 6. Electrical parameters of the hydrogen generator monitored during the test #3.

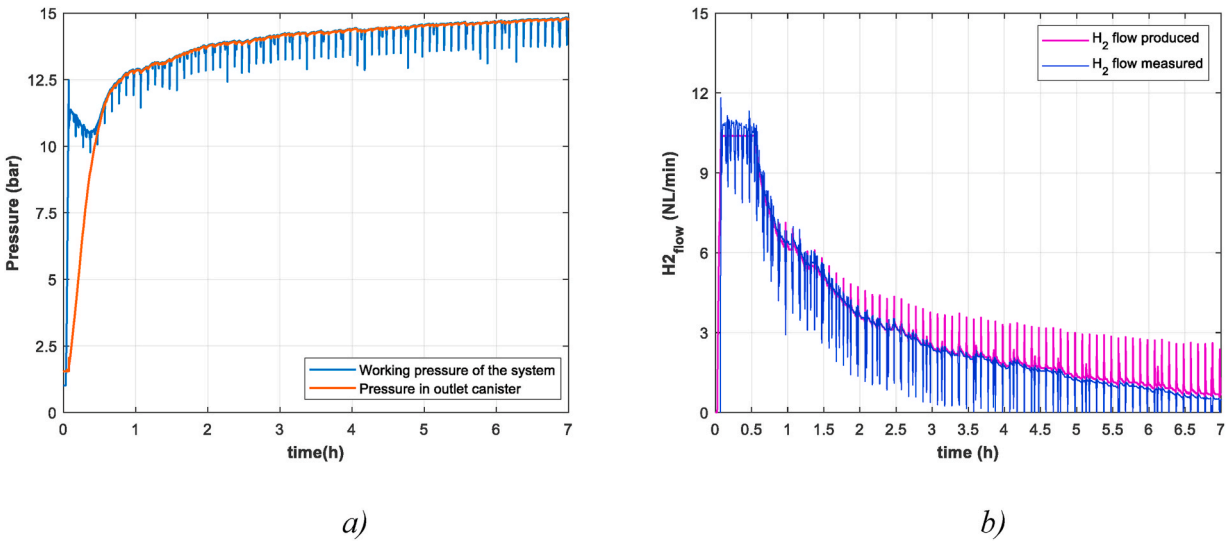

Fig. 7. Pressure and flow rate of the hydrogen produced by the generator during test #3.

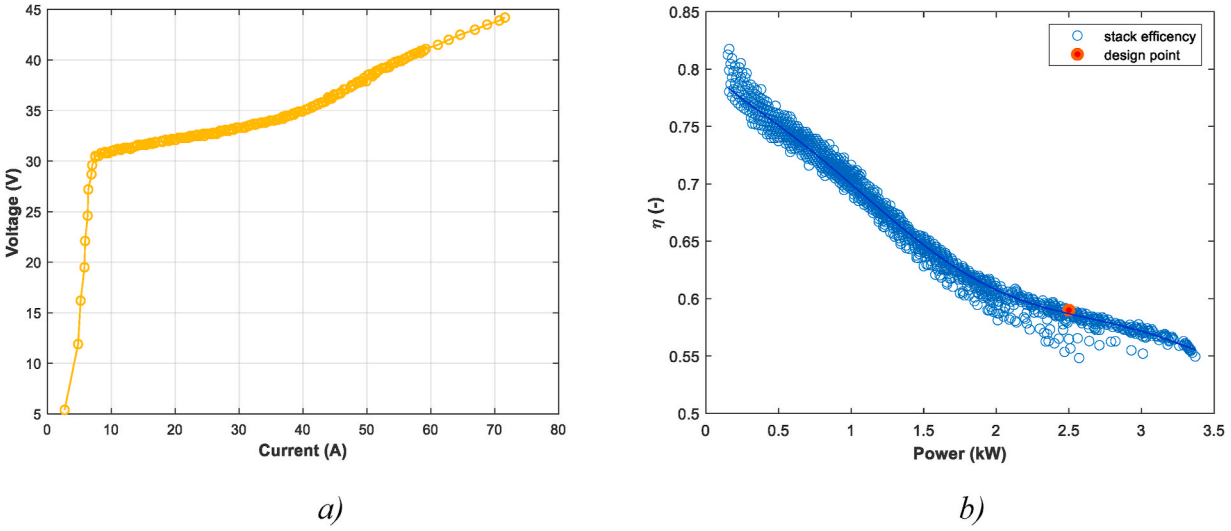

Fig. 8. Stack polarization curve and Efficiency curve obtained from experimental data for test #3.

In Fig. 8b is shown the efficiency curve of the stack during test #3, which looks very similar to the curve obtained in test #2 (Fig. 5b).

With the purpose of making an energy evaluation of the system, it is useful to look at the amount of hydrogen produced and stored as a result of the two tests under study. Fig. 9a represents the trends over time of the hydrogen produced and stored in the test performed in the absence of thermal conditioning (test #2). As can be seen at the end of the test there is a difference of about 5.2 g between the two masses ($m_{H2\_stored\_test\#2} = 59.0$ g, $m_{H2\_produced\_test\#2} = 64.2$ g), which is equal to the amount of hydrogen that is vented from the generator as a result of control logic and some possible losses along the pipes. From the information regarding the amount of hydrogen stored, it is possible to estimate the amount of energy stored by the MH storage system (Fig. 9b): at the end of test #2, about 2.00 kWh of energy was accumulated in the form of MH against the 3.25 kWh consumed by the stack electrolyzer, hence, as a result, it turns out that the mean stack efficiency is 61.5 %. These results can be compared with those concerning test #3 and shown in Fig. 9(c and d). It is evident that the cooling of MH tanks has a key role in the optimization of the storage system, and therefore in the PEM electrolyzer-MH coupling. Specifically, the mass of hydrogen stored, as well as the energy stored, is approximately twice the amount of hydrogen of test #2, namely $m_{H2\_stored\_test\#3}$ is equal to 119.0 g, corresponding to 3.90 kWh of energy stored in form of MH. On the other hand, also the energy consumed by the stack is much higher, namely equal to 6.35 kWh. Which means that the mean stack efficiency at the end of the test is about 61.4 %.

Therefore, the mean stack efficiency can be considered the same for both tests. However, considering that these systems are designed to recover surplus energy from renewables, for the same amount of intercepted electrical power available, it is desirable to have a system that produces as much hydrogen as possible. Hence, the cooling of MH tanks allows the optimal coupling between the electrolyzer and the storage system based on MH since it allows to store a greater amount of energy.

The final part of energy analysis was carried out only on test #3 since it was considered the most interesting among the tests performed. More specifically, the power adsorbed by the auxiliaries in the electrolyzer was also monitored during this test, so it was possible to calculate the total efficiency of the PEM-E as the load varied. Fig. 10a shows that for loads below 30 %, the power adsorbed by auxiliaries assumes a dominant role: although the stack efficiency is high, the total efficiency drops as the load decreases. These findings are consistent with those reported by Kotowicz et al. [27]. On the other hand, at medium-high loads the

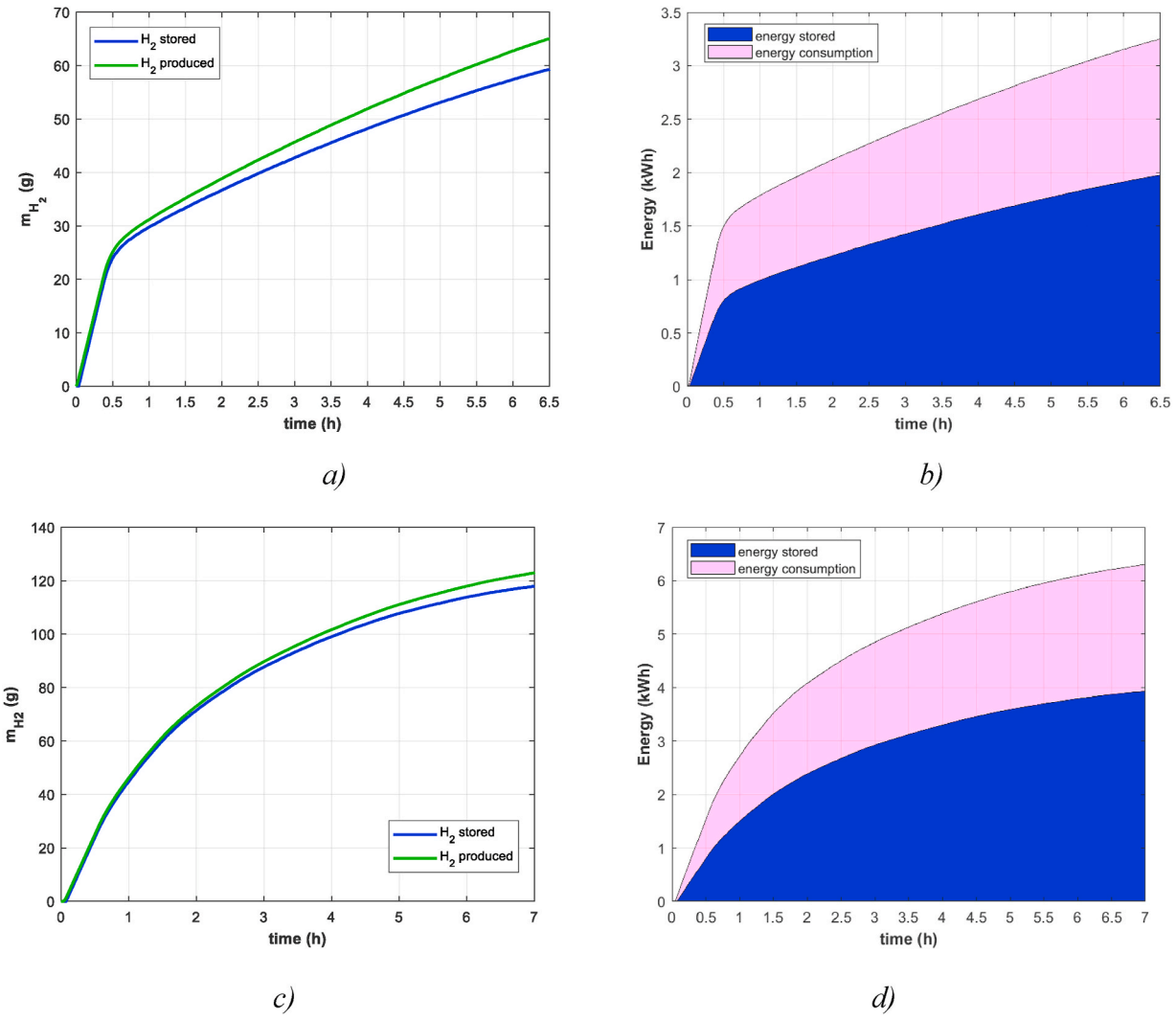

Fig. 9. Mass of hydrogen and equivalent energy produced and stored in test #2 and test #3.

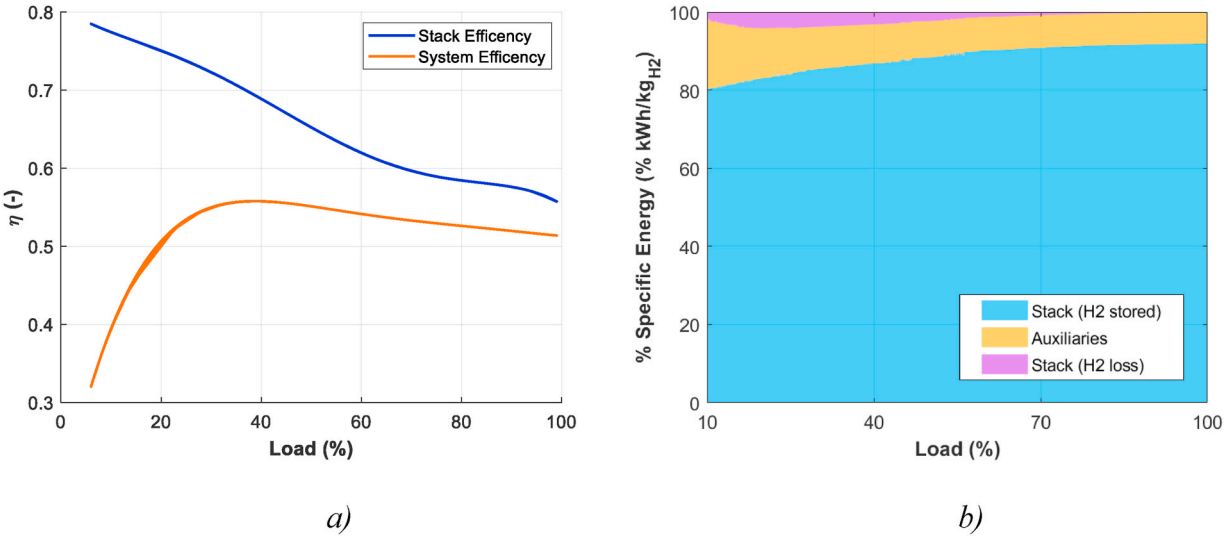

Fig. 10. Stack and system efficiency in test #3. Specific energy consumed by the stack in test #3. Specific energy consumed by the electrolyzer divided into three contributions as function of load.

leading role in efficiency calculation is assumed by the stack. Concurrently with efficiency, it is useful to refer to the specific energy of the system, which is the ratio of energy consumption to the mass of hydrogen produced by the generator. The specific energy consumed by the whole system can be defined as:

$$Specific\ Energy = \frac{E_{stack} + E_{Aux}}{m_{H2}} \quad (3)$$

Where E_{stack} is the energy consumed by the stack and E_{Aux} is the energy consumed by the auxiliaries.

However, since a part of hydrogen produced by the stack is lost due to the hydrogen vent logic, is important to consider also this aspect. Consequently, the electrolyzer specific energy consumption can be divided into two contributions: auxiliaries and stack, with the latter being split into two shares as is shown in Fig. 10b. As can be seen, the weight of the hydrogen vent is much more relevant at low load and aligns with the results reported by Landin and Windom [28].

3.3. Focus on PEM electrolyzer

As has been discussed so far, system performance can be affected by various boundary conditions, but also by characteristic behaviors affecting the individual components that make up the P2G system. The electrolyzer is one of the fundamental components of the system, so in this subchapter the effects on performance of two phenomena are studied in detail: hydrogen vent and current ripple.

3.3.1. Hydrogen vent logic

In order to ensure a high value of purity of hydrogen and water to be recirculated in the stack, a hydrogen ventilation strategy has been developed in the electrolyzer PLC to clean a filter located in the second stage of hydrogen separation. In more detail, the hydrogen purge is shown in Fig. 11, where the hydrogen flow and system pressure are represented as a function of time. As can be seen, whenever the system needs to purge hydrogen, the system pressure drops sharply causing an increase in the current sent to the stack (and thus in the flow of hydrogen produced), allowing the system to return to working pressure.

It is evident that the hydrogen purge occurs with a specific frequency along time. The opening of the purge valve occurs by following a specific timer that is set to 6 min and the estimate of the amount of hydrogen which is purged is almost constant and approximately 0.04 g for each pulse. Hence, if this control strategy occurs at low loads it is more penalizing in terms of system efficiency, than when the hydrogen generator operates at higher loads.

3.3.2. Ripple phenomena

In this work, the considered electrolyzer is supplied by the AC grid. The supply is divided into two parts: one for the auxiliaries and one for the stack. That of the auxiliaries is single-phase at 230 Vrms, while that of the stack is three-phase without neutral with a line-to-line voltage of 400 Vrms.

The interface between the stack and the grid is an AC/DC converter that takes the above-mentioned three-phase as input and can output a DC voltage of up to 300 V and a current of up to 75 A. The maximum electrical load of the stack is 3.5 kW; consequently, the converter is oversized for the application, which may have been a design choice intended to enhance the modularity of the machine.

Electrical measurements were made upstream and downstream of the AC/DC converter.

The acquisition of the waveforms was made using a Tektronix TDS2004B oscilloscope, while the time course of the electrical quantities, as mentioned above, was obtained from the PLC of the electrolyzer.

Fig. 12 shows the waveforms of the three main line currents on the AC grid and those of the voltage and current on the stack when the load is about 5 % of the maximum load. This point was chosen as the point at which the electrolyzer tends to work most of the time.

As can be seen, the input current to the converter in steady state conditions is very impulsive, while on the DC side the voltage is stable, and the current, in this case, has a ripple at a frequency of about 300 Hz. As can be seen from Fig. 12 the rms and the mean value of the current are basically the same, in fact the ripple factor Υ is around 1.

It is evident from the measurements made that the intensity of the ripple is very low at low loads, but its frequency is in the range that has been shown to be the most damaging to the stack. Based on these tests, it is therefore assumed that the converter has a diode bridge at its input to rectify the input voltage (AC/DC), followed by a buck converter (DC/DC) to bring the voltage to the level required to power the stack at the chosen operating point. If only a diode rectifier were present, the voltage on the stack would be higher than measured and would be a constant value.

Since the converter has already been built, therefore assuming that the existing structure will not be altered, to mitigate the ripple phenomenon one can intervene on the control of the converter, either by increasing the buck switching frequency or by trying to operate the buck, if of interleaved topology, at points where the ripple is naturally absent [29].

4. Conclusion

This study highlighted the significant potential of low pressure P2H systems equipped with MH for hydrogen storage. The experimental test-

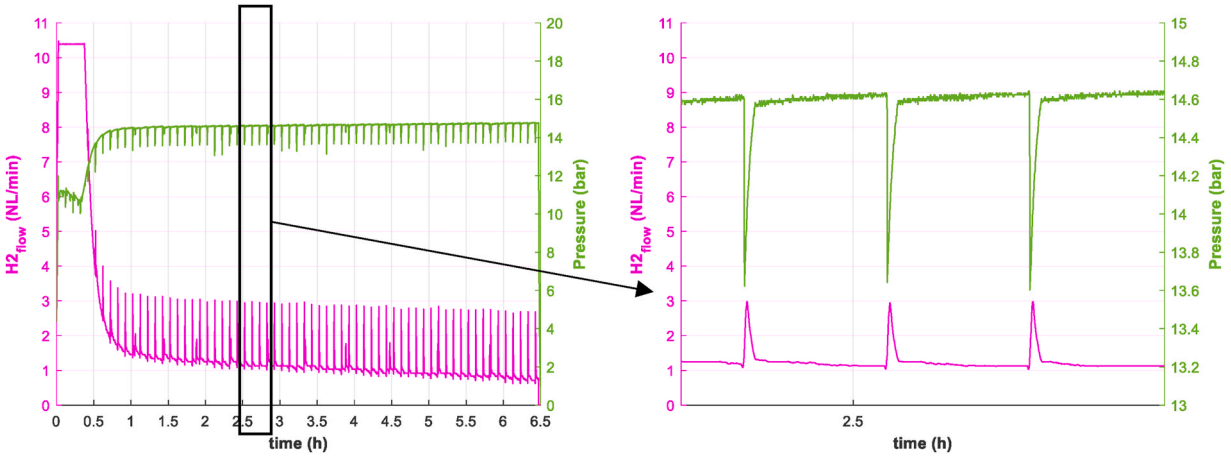

Fig. 11. Hydrogen vent actuation.

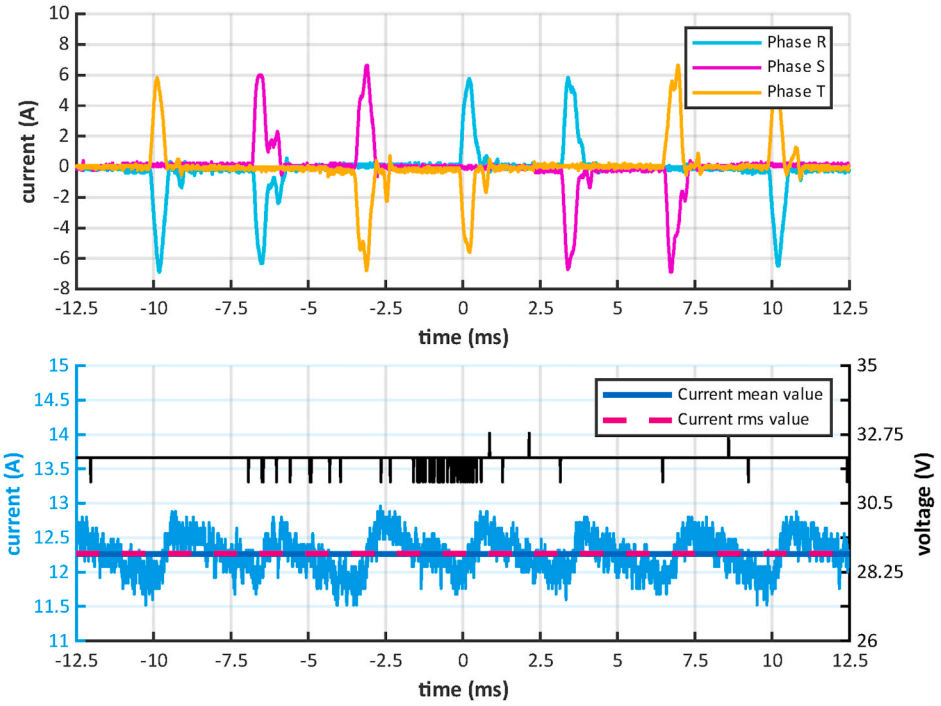

Fig. 12. Measured waveforms of current and voltage: on top the three-line input currents and on the bottom the voltage and current on the stack.

bench investigated in this study is represented by the coupling of a 2.5 kW PEM electrolyzer with AB2-type MH canisters. The experimental results demonstrated that several factors, including the size of the MH storage canisters and the effects of their thermal conditioning, play a crucial role in optimizing storage performance. The outcomes have shown that the larger canister (800 NL) is better suited with the considered electrolyzer size, in fact it can work at maximum load for much longer time, allowing to store more hydrogen and therefore maximizing the energy recover from renewables. The thermal conditioning of MH canisters is also essential to increase the efficiency of the MH storage, by facilitating the adsorption process. On the other hand, the power consumption of the cooling system should be taken into account to maximize the overall P2G efficiency, due to the extended duration of the hydrogen absorption process at low electrolyzer loads. It results that by using water within a cooling circuit to stabilize the temperature of the canisters around 20 °C during the test, a mean stack efficiency of 61.4 % is achieved.

The operational dynamics of the hydrogen generator, particularly concerning hydrogen venting and current ripple phenomena, due to the interaction of the PEM electrolyzer-MH tank direct coupling proved essential for improving the global efficiency of P2H systems. For instance, the hydrogen vent logic is much more penalizing for the system at low load, thus it is necessary to avoid this condition.

Future research will focus on conducting a more in-depth analysis of the venting logic, now performed at fixed time intervals (every 6 min). Subsequent studies will aim to develop a condition-based control logic, as opposed to a time-based approach, to enhance the hydrogen purge management of the PEM electrolyzer.

CRediT authorship contribution statement

Riccardo Alleori: Writing – review & editing, Writing – original draft, Visualization, Validation, Software, Project administration, Methodology, Investigation, Formal analysis, Data curation, Conceptualization. **Maria Alessandra Ancona:** Writing – review & editing, Supervision, Resources. **Michele Bianchi:** Writing – review & editing, Supervision, Funding acquisition. **Francesco Falcetelli:** Writing – review & editing, Writing – original draft, Visualization, Validation, Software, Project administration, Methodology, Investigation, Formal analysis, Data curation, Conceptualization. **Federico Ferrari:** Writing – review & editing, Writing – original draft, Visualization, Validation, Software, Project administration, Methodology, Investigation, Formal analysis, Data curation, Conceptualization. **Francesco Melino:** Writing – review & editing, Funding acquisition. **Paolo Pilati:** Writing – review & editing, Writing – original draft, Visualization, Validation, Software, Project administration, Methodology, Investigation, Formal analysis, Data curation, Conceptualization. **Mattia Ricco:** Writing – review & editing.

Declaration of competing interest

The authors declare that they have no known competing financial interests or personal relationships that could have appeared to influence the work reported in this paper.

Nomenclature

Acronyms

AC	Alternate Current
BoP	Balance of Plant
DAQ	Data Acquisition
DC	Direct Current
MH	Metal Hydride

P2H	Power-to-Hydrogen
P2G	Power-to-Gas
P2H2P	Power-to-Hydrogen-to-Power
P2G2P	Power-to-Gas-to-Power
PCT	Pressure-Composition-Temperature
PEM	Proton Exchange Membrane
PEM-E	Proton Exchange Membrane Electrolyzer
PLC	Programmable Logic Controller
RES	Renewable Energy Source
SOEC	Solid Oxide Electrolyzer Cells
TRL	Technology Readiness Level

Symbols

E	electric energy [J]
LHV	Lower Heating Value [J/kg]
m	mass [kg]
TiMg	Titanium–Magnesium alloy
X	current/voltage magnitude [A]

Greek Letters

η	efficiency [−]
γ	ripple factor [−]

Subscripts and superscripts

aux	auxiliaries
H2	hydrogen
m	mean
rms	root-mean-square
stack	electrolyzer stack

References

[1] Electrolysers - energy system - IEA. https://www.iea.org/energy-system/low-emission-fuels/electrolysers. [Accessed 16 October 2024].

[2] Risco-Bravo A, Varela C, Bartels J, Zondervan E. From green hydrogen to electricity: a review on recent advances, challenges, and opportunities on power-to-hydrogen-to-power systems. Renew Sustain Energy Rev Jan. 2024;189:113930. https://doi.org/10.1016/j.rser.2023.113930.

[3] Global hydrogen review 2024 – analysis - IEA. https://www.iea.org/reports/global-hydrogen-review-2024. [Accessed 20 November 2024].

[4] Hydrogen Europe. Clean hydrogen production pathways report. 2024 [Online]. Available: hydrogeneurope.eu.

[5] Flis G, Wakim G. Solid oxide electrolysis: a technology status assessment. 2023.

[6] Motealleh B, Liu Z, Masel RI, Sculley JP, Richard Ni Z, Meroueh L. Next-generation anion exchange membrane water electrolyzers operating for commercially relevant lifetimes. Int J Hydrogen Energy Jan. 2021;46(5):3379–86. https://doi.org/10.1016/j.ijhydene.2020.10.244.

[7] Usman MR. Hydrogen storage methods: review and current status. Renew Sustain Energy Rev Oct. 2022;167:112743. https://doi.org/10.1016/j.rser.2022.112743.

[8] Elberry AM, Thakur J, Santasalo-Aarnio A, Larmi M. Large-scale compressed hydrogen storage as part of renewable electricity storage systems. Int J Hydrogen Energy Apr. 2021;46(29):15671–90. https://doi.org/10.1016/j.ijhydene.2021.02.080.

[9] Zhang T, Uratani J, Huang Y, Xu L, Griffiths S, Ding Y. Hydrogen liquefaction and storage: recent progress and perspectives. Renew Sustain Energy Rev Apr. 2023;176:113204. https://doi.org/10.1016/j.rser.2023.113204.

[10] Ghaffari-Tabrizi F, Haemisch J, Lindner D. Reducing hydrogen boil-off losses during fuelling by pre-cooling cryogenic tank. Hydro Jun. 2022;3(2):255–69. https://doi.org/10.3390/hydrogen3020015.

[11] Klopčič N, Grimmer I, Winkler F, Sartory M, Trattner A. A review on metal hydride materials for hydrogen storage. J Energy Storage Nov. 2023;72:108456. https://doi.org/10.1016/j.est.2023.108456.

[12] Chibani A, et al. Impact of fins and cooling fluid on the hydrogenation process in a LaNi5-Based metal hydride reactor for hydrogen storage. Int J Hydrogen Energy Jun. 2024;69:134–46. https://doi.org/10.1016/j.ijhydene.2024.04.314.

[13] Førde Thomas. Theoretical and experimental studies of metal hydride storage units. Trondheim: Norwegian University of Science and Technology Department of Energy and Process Engineering; 2007.

[14] Nivedhitha KS, et al. Advances in hydrogen storage with metal hydrides: mechanisms, materials, and challenges. Int J Hydrogen Energy Apr. 2024;61:1259–73. https://doi.org/10.1016/j.ijhydene.2024.02.335.

[15] Drawer C, Lange J, Kaltschmitt M. Metal hydrides for hydrogen storage – identification and evaluation of stationary and transportation applications. J Energy Storage Jan. 2024;77:109988. https://doi.org/10.1016/j.est.2023.109988.

[16] Pasquini L, et al. Magnesium- and intermetallic alloys-based hydrides for energy storage: modelling, synthesis and properties. Prog. Energy Jul. 2022;4(3):032007. https://doi.org/10.1088/2516-1083/ac7190.

[17] Marangio F, Santarelli M, Cali M. Theoretical model and experimental analysis of a high pressure PEM water electrolyser for hydrogen production. Int J Hydrogen Energy Feb. 2009;34(3):1143–58. https://doi.org/10.1016/j.ijhydene.2008.11.083.

[18] Guilbert D, Vitale G. Experimental validation of an equivalent dynamic electrical model for a proton exchange membrane electrolyzer. In: 2018 IEEE international conference on environment and electrical engineering and 2018 IEEE industrial and commercial power systems europe (EEEIC/I&CPS europe). Palermo: IEEE; Jun. 2018. p. 1–6. https://doi.org/10.1109/EEEIC.2018.8494523.

[19] Kim J, Lee I, Tak Y, Cho BH. Impedance-based diagnosis of polymer electrolyte membrane fuel cell failures associated with a low frequency ripple current. Renew Energy Mar. 2013;51:302–9. https://doi.org/10.1016/j.renene.2012.09.053.

[20] Jarry T, et al. Impact of high frequency current ripples on the degradation of high-temperature PEM fuel cells (HT-PEMFC). Int J Hydrogen Energy Jun. 2023;48(54):20734–42. https://doi.org/10.1016/j.ijhydene.2023.03.027.

[21] Zhan Y, Guo Y, Zhu J, Liang B, Yang B. Comprehensive influences measurement and analysis of power converter low frequency current ripple on PEM fuel cell. Int J Hydrogen Energy Nov. 2019;44(59):31352–9. https://doi.org/10.1016/j.ijhydene.2019.09.231.

[22] Buitendach HPC, Gouws R, Martinson CA, Minnaar C, Bessarabov D. Effect of a ripple current on the efficiency of a PEM electrolyser. Results in Engineering Jun. 2021;10:100216. https://doi.org/10.1016/j.rineng.2021.100216.

[23] Valdez-Resendiz JE, Rosas-Caro JC, Sanchez VM, Lopez-Nuñez AR. Experimental study of a fuel cell stack performance operating with a power electronics converter with high-frequency current ripple. Int J Hydrogen Energy Jan. 2024. https://doi.org/10.1016/j.ijhydene.2024.01.248.

[24] Heliocentris Academia International GmbH, 'Metal Hydride Storage Canisters' [Online]. Available: https://www.heliocentrisacademia.com/metal-hydride-storage-canisters/p1522?currency=usd.

[25] Keddar M, Zhang Z, Periasamy C, Doumbia ML. Power quality improvement for 20 MW PEM water electrolysis system. Int J Hydrogen Energy Dec. 2022;47(95):40184–95. https://doi.org/10.1016/j.ijhydene.2022.08.073.

[26] Mohanpurkar Manish, et al. Electrolyzers enhancing flexibility in electric grids. Energies Nov. 2017;10(11):1836. https://doi.org/10.3390/en10111836.

[27] Kotowicz J, Bartela Ł, Węcel D, Dubiel K. Hydrogen generator characteristics for storage of renewably-generated energy. Energy Jan. 2017;118:156–71. https://doi.org/10.1016/j.energy.2016.11.148.
[28] Landin NK, Windom BC. Evaluating the efficiency of a proton exchange membrane green hydrogen generation system using balance of plant modeling. Int J Hydrogen Energy Feb. 2024;57:1273–85. https://doi.org/10.1016/j.ijhydene.2024.01.128.
[29] Drobnic K, et al. An output ripple-free fast charger for electric vehicles based on grid-tied modular three-phase interleaved converters. IEEE Trans Ind Appl Nov. 2019;55(6):6102–14. https://doi.org/10.1109/TIA.2019.2934082.